

**NITROGEN-SULFUR AND NITROGEN-BORON
CO-DOPED BIOCHAR AS
PEROXYMONOSULFATE ACTIVATOR FOR
FLUOROQUINOLONE ANTIBIOTICS
REMOVAL**

CHOONG ZHENG YI

UNIVERSITI SAINS MALAYSIA

2023

**NITROGEN-SULFUR AND NITROGEN-BORON
CO-DOPED BIOCHAR AS
PEROXYMONOSULFATE ACTIVATOR FOR
FLUOROQUINOLONE ANTIBIOTICS
REMOVAL**

by

CHOONG ZHENG YI

**Thesis submitted in fulfilment of the requirements
for the degree of
Master of Science**

February 2023

ACKNOWLEDGEMENT

First and foremost, I would like to express my deepest appreciation towards my supervisor, Dr. Oh Wen Da for providing me with a lot of insightful and profound comments in the course of my research. His patient guidance had been inspiring to me and without them, I would not have completed my Master's programme easily. I also would like to thank my senior, Mohamed Faisal Gasim, in providing help and advice whenever I faced difficulties in my studies. I would also like to express my gratitude to Dr. Mohd. Hazwan Hussin for allowing me to use his potentiostat, and Tuan Sherwyn Hamidon for guiding me in my electrochemical studies.

I would also like to thank the School of Chemical Sciences, Universiti Sains Malaysia (USM) for providing the spaces and various facilities for me to carry out my studies. I would also like to thank the technical and the administrative staffs in helping and facilitating my studies. I would like to thank the Fundamental Research Grant Scheme with project code FRGS/1/2020/STG04/USM/02/2 and GRA-Assist (2020) for providing financial support that really help relieve my financial burden during my Master's Programme.

Last but not least, I would like to express my sincerest gratitude to my parents for their love and support throughout my Master's Programme. I would also like to thank my friend, Mr. Ma Yik Ken, for his help throughout my studies.

TABLE OF CONTENTS

ACKNOWLEDGEMENT	ii
TABLE OF CONTENTS	iii
LIST OF TABLES	vii
LIST OF FIGURES	viii
LIST OF SYMBOLS, ABBREVIATION AND NOMENCLATURES	xi
LIST OF APPENDICES	xiii
ABSTRAK	xiv
ABSTRACT	xvi
CHAPTER 1 INTRODUCTION	1
1.1 Background.....	1
1.2 Problem statement and hypothesis.....	5
1.3 Objectives and scope of study.....	8
1.4 Organization of thesis.....	9
CHAPTER 2 LITERATURE REVIEW	11
2.1 Fundamentals of catalytic peroxymonosulfate activation.....	11
2.2 Carbocatalyst.....	12
2.2.1 Graphene-based materials.....	13
2.2.2 Carbon nanotubes.....	14
2.2.3 Ordered mesoporous carbon.....	15
2.2.4 Nanodiamond.....	16
2.2.5 Amorphous Carbon.....	16
2.3 General properties of carbocatalyst for PMS activation.....	17
2.4 Effects of single heteroatom-doped carbocatalysts in PMS activation.....	20
2.4.1 Nitrogen doping.....	20
2.4.2 Boron doping.....	22
2.4.3 Phosphorus doping.....	23
2.4.4 Sulfur doping.....	23

2.4.5	Others.....	24
2.5	Effect of multi-heteroatom-doped carbocatalyst in PMS activation.....	24
2.5.1	Dual-heteroatom-doped carbocatalyst.....	25
2.5.2	Multi-heteroatom-doped carbocatalyst.....	36
2.6	Performance of multi-heteroatom-doped carbocatalyst.....	37
2.7	General considerations for the preparation of N, S- and N, B-co-doped biochar.....	46
2.8	Summary of the literature review.....	49
CHAPTER 3 MATERIALS AND RESEARCH METHODOLOGY.....		50
3.1	Experiment Outline.....	50
3.2	Chemicals and materials.....	51
3.3	Synthesis of carbocatalysts.....	52
3.2.1	Synthesis of nitrogen, sulfur co-doped biochar.....	52
3.2.2	Synthesis of nitrogen, boron co-doped biochar.....	53
3.4	Characterization of the carbocatalysts.....	55
3.4.1	Field-emission scanning electron microscope (FESEM) equipped with electron dispersive spectroscopy (EDX).....	55
3.4.2	High Resolution Transmission Electron Microscopy (HR-TEM).....	55
3.4.3	X-ray diffraction (XRD) analysis.....	56
3.4.4	Nitrogen gas adsorption-desorption analysis.....	56
3.4.5	Fourier Transform Infrared (FTIR) Spectroscopy.....	56
3.4.6	Raman spectroscopy.....	57
3.4.7	CHNS elemental analysis.....	57
3.4.8	X-ray Photoelectron Spectroscopy (XPS).....	57
3.5	Performance studies.....	58
3.5.1	Performance of nitrogen, sulfur co-doped biochar as PMS activator for gatifloxacin removal.....	58
3.5.2	Performance of nitrogen, boron co-doped biochar as PMS activator for ciprofloxacin removal.....	59
3.6	Analytical method.....	60
3.6.1	Pollution concentration determination.....	60

3.6.2	Peroxymonosulfate concentration determination.....	61
3.6.3	Kinetic model development.....	61
3.6.4	Electrochemical studies.....	62
3.6.5	Degradation pathway determination, total organic carbon and toxicity evaluation.....	63
CHAPTER 4 NITROGEN, SULFUR-CO-DOPED BIOCHAR AS PEROXYMONOSULFATE ACTIVATOR FOR GATIFLOXACIN REMOVAL.....		65
4.1	Introduction.....	65
4.2	Results and discussion.....	65
4.2.1	Characteristics and formation of BSN-T catalysts.....	65
4.2.2	Performance and kinetics study.....	72
4.2.3	Identification of major reactive species.....	83
4.2.4	Proposed PMS activation pathway.....	87
4.2.5	Proposed GAT degradation pathway and toxicity study.....	90
4.3	Conclusion.....	94
CHAPTER 5 NITROGEN, BORON-CO-DOPED BIOCHAR AS PEROXYMONOSULFATE ACTIVATOR FOR CIPROFLOXACIN REMOVAL.....		96
5.1	Introduction.....	96
5.2	Results and discussion.....	97
5.2.1	Characterization of the carbocatalysts.....	97
5.2.2	Performance studies.....	103
5.2.3	Identification of dominant RS and proposed PMS activation pathway.....	110
5.2.4	Degradation pathway and toxicity assessment.....	115
5.3	Conclusion.....	119
CHAPTER 6 CONCLUSION AND RECOMMENDATIONS.....		121
6.1	Conclusion.....	121
6.2	Recommendations for future study.....	122
6.2.1	Mechanistic studies of multi-heteroatom-doped carbocatalyst in peroxymonosulfate activation.....	122
6.2.2	Explore various synthesis methods/parameters for multi- heteroatom-doped carbocatalyst.....	123

6.2.3	Application of multi-heteroatom-doped carbocatalyst in water remediation via peroxymonosulfate activation.....	125
REFERENCES		128
APPENDICES		
LIST OF PUBLICATIONS		

LIST OF TABLES

		Page
Table 1.1	Advantages and disadvantages of various wastewater treatment methods.....	3
Table 2.1	Characteristics of catalyst and enhancement strategies for improved catalytic activity.....	19
Table 2.2	Characteristics, performance, and active sites of various multi-heteroatom-doped carbocatalyst for PMS activation ('*' marks lower efficiency after co-doping).....	39
Table 3.1	List of chemicals used.....	51
Table 3.2	Naming of BSN-Ts.....	53
Table 3.3	Naming of NB-BCs.....	54
Table 3.4	Mobile phase compositions used in the elution gradient mode.....	64
Table 4.1	Rate constants for the effect of catalyst loading and PMS dosage in pseudo-first order kinetic and current kinetic model ($[GAT] = 8 \text{ mg L}^{-1}$; $\text{pH } 3$).....	78
Table 4.2	Rate constants for the effect of pH in pseudo-first order kinetic and current kinetic model ($[GAT] = 8 \text{ mg L}^{-1}$; $[Cat] = 0.10 \text{ g L}^{-1}$; $[PMS] = 0.40 \text{ g L}^{-1}$).....	80
Table 4.3	Rate constants for the reusability of BSN-800 in pseudo-first order kinetic and current kinetic model ($[GAT] = 8 \text{ mg L}^{-1}$; $[Cat] = 0.10 \text{ g L}^{-1}$; $[PMS] = 0.40 \text{ g L}^{-1}$; $\text{pH} = 3$).....	81
Table 4.4	Rate constants for the performance at different water matrices of BSN-800 in pseudo-first order kinetic and current kinetic model. ($[GAT] = 8 \text{ mg L}^{-1}$; $[Cat] = 0.10 \text{ g L}^{-1}$; $[PMS] = 0.40 \text{ g L}^{-1}$; $\text{pH} = 3$).....	83

LIST OF FIGURES

		Page
Figure 1.1	(a) General structure for fluoroquinolone antibiotics, and (b) some common examples of fluoroquinolone antibiotics.....	1
Figure 2.1	Reaction mechanism involving radical and nonradical pathway during PMS activation.....	12
Figure 2.2	The structures of various carbon allotropes, (a) graphene, (b) reduction process from graphene oxide to reduced graphene oxide, (c) carbon nanotubes, (d) synthesis of ordered mesoporous carbon by using template route, and (e) nanodiamond.....	13
Figure 2.3	Effect of various heteroatoms on PMS activation.....	20
Figure 2.4	The possible interactions of N and S moieties in a confined carbon structure.....	26
Figure 2.5	The possible interactions of N and B moieties in the confined carbon structure.....	28
Figure 2.6	The possible interactions of N and P moieties in the confined carbon structure.....	30
Figure 2.7	The possible interactions of N and halogen, and active sites of various combinations of heteroatoms.....	33
Figure 2.8	Influence of the doping sequence on the preparation of N, S-co-doped carbocatalyst.....	48
Figure 3.1	Outline of the studies.....	50
Figure 3.2	Schematic diagram for synthesis of BSN-Ts.....	53
Figure 3.3	Schematic diagram for preparation of NB-BCs.....	54
Figure 3.4	Performance study (batch study) of the carbocatalysts in PMS activation.....	58
Figure 3.5	The preparation of carbocatalyst coated FTO electrode.....	63
Figure 4.1	(a) XRD patterns, (b) Raman spectra of various BSN-Ts.....	67
Figure 4.2	The proposed mechanism of formation of BSN-T.....	67

Figure 4.3	(a) FESEM micrograph, (b) EDX elemental mapping and (c)-(e) TEM micrograph of BSN-800.....	69
Figure 4.4	(a) Nitrogen adsorption-desorption isotherms, and (b) FTIR spectra of various BSN-Ts.....	70
Figure 4.5	High resolution XPS spectra of BSN-Ts for (a) N 1s and (b) S 2p.....	72
Figure 4.6	Chemical compositions of BSN-Ts.....	72
Figure 4.7	Effects of (a) catalyst type (different synthesis temperature and single-doped biochar), and (b) mode of operation on GAT degradation via PMS activation.....	74
Figure 4.8	Performances at various catalyst loadings and PMS dosages with (a,c,e,g) GAT concentration against time, (b,d,f,h) PMS concentration against time (dotted line: pseudo-first order kinetic model, solid line: current kinetic model).....	77
Figure 4.9	Effect of pH on (a) GAT removal, and (b) PMS consumption by BSN-800/PMS system(dotted line: pseudo-first order kinetics, solid line: proposed kinetic model).....	79
Figure 4.10	(a) GAT removal and (b) PMS consumption for reusability by BSN-800/PMS system (dotted line: pseudo-first order kinetics, solid line: proposed kinetic model).....	81
Figure 4.11	(a) GAT removal and (b) PMS consumption in real water matrices by BSN-800/PMS system (dotted line: pseudo-first order kinetics, solid line: proposed kinetic model).....	82
Figure 4.12	Effect of chemical scavengers on (a) GAT removal and (b) PMS consumption by BSN-800/PMS system.....	84
Figure 4.13	(a) Electrochemical impedance spectra, (b) Linear sweep voltammetry, (c) chronopotentiometry (inlet: chronoamperometry), and degradation of GAT (d) with/without premixing of GAT and (e) with D2O in the catalytic BSN-800/PMS system.....	87
Figure 4.14	XPS spectra of used BSN-800 at the (a) survey scan, (b) N 1s, and (c) S 2p regions.....	88
Figure 4.15	The proposed PMS activation mechanism by BSN-800.....	90
Figure 4.16	Proposed degradation pathway of GAT in the catalytic PMS activation system by BSN-800.....	93

Figure 4.17	(a) Acute toxicity, (b) developmental toxicity, (c) bioconcentration factor, (d) mutagenicity of GAT and its degradation intermediates (* indicates no available data).....	94
Figure 5.1	(a) XRD patterns, (b) Raman spectra, (c) N ₂ adsorption-desorption isotherms, (d) FTIR spectra of the as-prepared carbocatalysts.....	98
Figure 5.2	(a) FESEM micrograph, and (b) EDX mapping of NB-BC-1...	100
Figure 5.3	High resolution XPS spectra for (a) N 1s and (b) B 1s of the carbocatalysts.....	100
Figure 5.4	Heteroatom doping mechanism of NB-BCs.....	102
Figure 5.5	Effects of different (a) carbocatalysts, (b) catalyst loadings, (c) PMS dosages, and (d) initial pHs on CIP degradation in NB-BC-1/PMS system.....	105
Figure 5.6	Effects of (a) various dissolved matters, and different concentrations of (b) NO ₃ ⁻ , (c) humic acid, and (d) Cl ⁻ at various concentrations on CIP removal by NB-BC-1/PMS system.....	108
Figure 5.7	(a) Application of NB-BC-1/PMS system in real water matrices, and (b) reusability of NB-BC-1.....	110
Figure 5.8	(a) Scavenger studies, (b) electrochemical impedance spectra, (c) electrochemical impedance spectra, and (d) chronopotentiometry of NB-BC-1.....	112
Figure 5.9	High resolution XPS spectra of used NB-BC-1 for a) N 1s, and b) B 1s.....	115
Figure 5.10	Proposed PMS activation by NB-BC-1 via radical and nonradical pathway.....	115
Figure 5.11	Proposed CIP degradation pathways in the catalytic PMS activation system by NB-BC-1.....	118
Figure 5.12	(a) Acute toxicity, (b) development toxicity, (c) bioconcentration factor, (d) mutagenicity of GAT and its degradation intermediates (* indicate no available data).....	119
Figure 6.1	Diagram of the continuous flow treatment mode.....	126

LIST OF SYMBOLS, ABBREVIATIONS AND NOMENCLATURES

ACT	Acetaminophen
AOPs	Advance oxidation processes
BA	Boric acid
BET	Brunauer-Emmett-Teller
BP-4	Benzophenone-4
BPA	Bisphenol A
CA	Chronoamperometry
CIP	Ciprofloxacin
CNTs	Carbon nanotubes
CP	Chronopotentiometry
DFT	Density functional theory
EDX	Electron dispersive spectroscopy
EIS	Electrochemical impedance spectroscopy
ESI	Electrospray ionization
FESEM	Field-emission scanning electron microscope
FLQ	Fluoroquinolone
FTIR	Fourier transfer infrared spectroscopy
GAT	Gatifloxacin
HR-TEM	High resolution-transmission electron microscopy
LSV	Linear sweep voltammetry
MB	Methylene blue
MET	Metolachlor
MP	Methyl paraben
ND	Nanodiamond

OMC	Ordered mesoporous carbons
ORR	Oxygen reduction reaction
PDS	Peroxydisulfate
PMS	Peroxymonosulfate
PS	Persulfates
RS	Reactive species
rGO	Reduced graphene oxide
RhB	Rhodamine B
SR-AOPs	Sulfate-based advance oxidation processes
SAM	Sulfacetamide
SCE	Standard calomel electrode
SMX	Sulfamethoxazole
SSA	Specific surface area
TBA	Tert-butyl alcohol
TOC	Total organic carbon
XPS	X-ray photoelectron spectroscopy
XRD	X-ray diffraction

LIST OF APPENDICES

- APPENDIX A Effects of sawdust:urea:thiourea mass ratio.
- APPENDIX B FESEM micrograph of (a) BC-600 and (b) BSN-600.
- APPENDIX C EDX elemental mapping of (a) BSN-600, (b) BSN-700, and (c) wt.% of C, N and S of BSN-Ts.
- APPENDIX D Pseudo-first order rate constant for GAT removal (20 min reaction time) at various catalyst loadings and PMS dosages.
- APPENDIX E The pH drift method for determining the point of zero charge of BSN-800.
- APPENDIX F Mass spectra at different retention times for GAT intermediates identification.
- APPENDIX G EDX mapping of (a) B-BC-1, (b) N-BC, (c) NB-BC-2, and (d) NB-BC-3, and (e) Elemental composition of the carbocatalyst.
- APPENDIX H pH drift method of NB-BC-1.
- APPENDIX I LC/MS spectrum for intermediates identifications at different retention time.

**BIOARANG KOTERDOP NITROGEN-SULFUR DAN NITROGEN-BORON
SEBAGAI PENGAKTIF PEROXIMONOSULFAT BAGI PENYINGKIRAN
ANTIBIOTIK FLUOROKUINOLON**

ABSTRAK

Baru-baru ini, aplikasi karbomangkin koterdop dua heteroatom dalam proses pengoksidaan lanjutan berasaskan peroximonosulfat (PMS) untuk menyingkirkan bahan pencemar keras telah semakin dikaji. Memandangkan kajian tentang karbomangkin koterdop dua heteroatom dalam pengaktifan PMS masih baru, objektif utama kajian ini adalah untuk mengkaji pelbagai bioarang koterdop dua heteroatom untuk pengaktifan PMS. Dalam bahagian pertama kajian (Bab 4), satu siri bioarang koterdop N-S (BSN-Ts) pada suhu berbeza telah disediakan menggunakan kaedah pengkalsinan satu langkah. Melalui pelbagai pencirian, didapati bahawa $g\text{-C}_3\text{N}_4$ terbentuk dahulu melalui pempolimeran urea dan tiourea, dan menelan bioarang. Pada suhu sintesis yang lebih tinggi, $g\text{-C}_3\text{N}_4$ terurai dan bergabung dengan biochar, membentuk BSN-Ts. Prestasi BSN-Ts sebagai pengaktif PMS untuk penyingkiran gatifloksasin (GAT) telah dinilai dan didapati bahawa BSN-Ts yang disediakan pada $800\text{ }^\circ\text{C}$ (BSN-800) menunjukkan prestasi yang paling tinggi kerana luas permukaan spesifiknya yang agak tinggi ($S_{\text{BET}} = 419\text{ m}^2\text{ g}^{-1}$) dan sinergi antara heteroatom. Model kinetik berdasarkan penggunaan PMS tertib kedua dan penyingkiran GAT tertib pertama telah dibentuk bagi menerangkan sistem degradasi pada pelbagai keadaan operasi (cth pemuatan BSN-800, dos PMS dan pH). Walaupun meningkatkan dos PMS boleh menggalakkan penyingkiran GAT, k_{PMS} dan k' telah dikurangkan kerana utiliti PMS yang tidak cekap. Peningkatan muatan BSN-800 boleh meningkatkan k_{PMS} dan k' sebanyak 3.3 – 6.3 dan 1.5 – 4.6 kali ganda, menunjukkan muatan mangkin yang

lebih tinggi adalah lebih diingini berbanding dengan dos PMS yang lebih tinggi. Daripada kajian scavenger dan kajian elektrokimia, adalah dicadangkan bahawa laluan bukan radikal (penjanaan $^1\text{O}_2$ dan mekanisme mediator elektron) ialah laluan pengaktifan PMS utama dengan grafitik N dan tiofenik S bertindak sebagai tapak aktif. Walaupun mempunyai kebolegunaan semula yang terhad, BSN-800 boleh berfungsi dengan baik dalam pelbagai matriks air (dengan >70% penyingkiran GAT dalam 1 h). Akhir sekali, laluan degradasi GAT telah dicadangkan berdasarkan molekul perantaraan degradasi yang dikenalpasti. Dalam bahagian kedua kajian (Bab 5), satu siri bioarang koterdop N-B (NB-BCs) telah disediakan melalui proses pengkalsinan dua langkah dengan asid borik (BA): nisbah jisim urea yang berbeza-beza. Melalui pelbagai pencirian, didapati pengedopan B dahulu boleh memudahkan pengedopan N melalui interaksi gugusan B dengan NH_3 . Prestasi NB-BC sebagai pengaktif PMS telah dinilai dan didapati bahawa NB-BC-1 (BA:nisbah jisim urea = 0.025: 1) menunjukkan prestasi yang terbaik dalam penyingkiran siprofloksasin (CIP) (dengan $k_{app} = 0.053 \text{ min}^{-1}$). Ia juga didapati bahawa pengaktifan PMS oleh NB-BC-1 boleh dipengaruhi oleh dos PMS, muatan mangkin dan pH. Walaupun kebanyakan bahan terlarut menunjukkan kesan perencatan dalam penyingkiran CIP disebabkan kesan penghapusan oleh bahan terlarut, Br^- boleh meningkatkan penyingkiran CIP dengan ketara disebabkan oleh pembentukan RS sekunder yang lebih reaktif melalui tindak balas Br^- dengan $\text{SO}_4^{\bullet-}$. Kajian juga menunjukkan bahawa NB-BC-1 boleh mengaktifkan PMS melalui kedua-dua laluan radikal dan bukan radikal. Akhir sekali, laluan degradasi CIP juga dicadangkan berdasarkan perantaraan degradasi yang dikenal pasti. Secara keseluruhan, kajian ini memberikan pandangan berharga tentang mekanisme pembentukan bioarang koterdop dua heteroatom dan mekanisme pengaktifan PMS.

**NITROGEN-SULFUR AND NITROGEN-BORON CO-DOPED BIOCHAR AS
PEROXYMONOSULFATE ACTIVATOR FOR FLUOROQUINOLONE
ANTIBIOTICS REMOVAL**

ABSTRACT

Recently, the application of multi-heteroatom-doped carbocatalyst in peroxymonosulfate (PMS)-based advanced oxidation processes for removing recalcitrant pollutant has been increasingly studied. As the studies on multi-heteroatom-doped carbocatalyst in PMS activation is still nascent, the main objective of this study is to study various multi-heteroatom-doped biochar for PMS activation. In the first part of the study (Chapter 4), a series of N, S-co-doped biochar (BSN-Ts) were prepared at different temperature using one-step calcination method. Through various characterization, it was found that g-C₃N₄ was first formed by polymerization of urea and thiourea, and engulf the biochar. At higher synthesis temperature, the g-C₃N₄ decomposed and coalesce with the biochar, forming BSN-Ts. The performance of BSN-Ts as PMS activators for gatifloxacin (GAT) removal were evaluated and were found that BSN-Ts prepared at 800 °C (BSN-800) showed the greatest performance due to its relatively high specific surface area ($S_{\text{BET}} = 419 \text{ m}^2 \text{ g}^{-1}$) and synergism between heteroatoms. A kinetic model based on the second-order PMS consumption and first-order GAT removal was developed to describe the degradation systems at various operating conditions (e.g. BSN-800 loading, PMS dosage and pH). It was found that despite having promoted GAT removal, increasing PMS dosage can decrease the k_{PMS} and k' due to the inefficient utility of PMS. The increase of catalyst loadings can increase the k_{PMS} and k' by 3.3 – 6.3 and 1.5 – 4.6 times, showing higher catalyst loadings is more desirable compared to having higher PMS dosage. From the

scavenger studies and electrochemical studies, it is proposed that nonradical pathway ($^1\text{O}_2$ generation and electron mediator mechanisms) is the major PMS activation pathway with graphitic N and thiophenic S acting as the active sites. Despite having limited reusability, BSN-800 can perform well in various water matrixes (with >70% GAT removal in one hour). Lastly, the GAT degradation pathway was proposed based on the identified degradation intermediates. In the second part of the study (Chapter 5), a series of N, B-co-doped biochar (NB-BCs) were synthesized using two-steps calcination process with varying boric acid (BA):urea mass ratio. Through various characterizations, it was found that pre-doping of B can facilitate N doping through interaction of the B moieties with NH_3 . The performance of NB-BCs as PMS activators were evaluated and the results showed that NB-BC-1 (BA:urea mass ratio = 0.025:1) performed the best in ciprofloxacin (CIP) removal (with $k_{app} = 0.053 \text{ min}^{-1}$). It was also found that the PMS activation by NB-BC-1 can be affected by PMS dosages, catalyst loadings and initial pHs. While most dissolved matters showed inhibitory effect in CIP removal due to the scavenging effect by the dissolved matters, Br^- can significantly improve the CIP removal due to the formation of more reactive secondary RS by reaction of Br^- with $\text{SO}_4^{\bullet-}$. It was also found that NB-BC-1 activates PMS through both radical and nonradical pathway. Lastly, the CIP degradation pathway was also proposed based on the identified degradation intermediates. Overall, this study provides valuable insights into the multi-heteroatom-doped biochar formation mechanism and the PMS activation mechanism.

CHAPTER 1

INTRODUCTION

1.1 Background

Environmental pollution by pharmaceutical wastes such as antibiotics poses a major threat to the ecosystem and public health alike. As the applications of antibiotics expand, antibiotics are increasingly detected in various water bodies [1, 2]. Fluoroquinolone (FLQ) antibiotics (shown in **Figure 1.1**) is a class of antibiotics that are used to treat various bacterial infections including skin, respiratory and tissue infections. Among the FLQ antibiotics, ciprofloxacin (CIP) and gatifloxacin (GAT) were widely used in various applications. While both CIP and GAT were generally used to treat various bacterial infections including upper and lower respiratory infections, skin and soft tissue infections and pneumonia [3, 4], they have different activities towards different bacterial species and hence they were used separately depending on the patients' circumstances [4]. Due to its rampant usages in many fields, they have been detected in wastewater and river, which can potentially pose threat to human health and disrupt the ecosystem. For instance, trace quantities of the antibiotics that were leaked into the environment can cause development of resistance strain among the bacteria [5, 6], leading to increased treatment difficulty, costs and mortality rate. While in Malaysia, CIP and GAT were detected in various water bodies such as river water to wastewater [7, 8]. For instance, CIP concentration of 112.40 to 198.91 ng L⁻¹ were detected in different river water across Selangor, which these CIP concentration can potentially cause adverse effect to adults and children's health [7]. Furthermore, the presence of CIP and GAT resistance genes among various bacterial species were detected in various water bodies in Malaysia [9]. Hence, the removal of

FLQ antibiotics in the wastewater is vitally important to prevent the alleviation of antibiotics pollution in Malaysia.

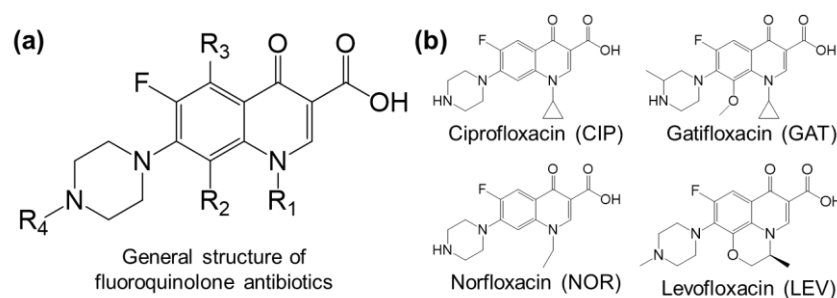


Figure 1.1. (a) General structure for FLQ antibiotics, and (b) some common examples of FLQ antibiotics.

To reduce the release of FLQ antibiotics into the environment, various methods including adsorption, membrane filtration, biodegradation and advance oxidation processes (AOPs) were investigated for treating the wastewater. The advantages and disadvantages of these methods are summarized in **Table 1.1**. While adsorption and membrane filtration have a relatively simple operational procedure when compared with other treatment methods, they may produce secondary pollution, which potentially limit their practical applications. Furthermore, adsorption is an equilibrium reliant process, which the adsorption process will ultimately be stopped once the adsorbent reached its adsorption capacity. On the other hand, biodegradation have been used as a mean to degrade FLQ antibiotics [10, 11]. For instance, Manasfi et al. [10] has shown that *Trichoderma* fungi are efficient in degrading a variety of FLQ antibiotics such as CIP and ofloxacin. However, biological treatments generally require longer treatment time (usually takes up to days), require delicate maintenance of the sludges and sometimes are ineffective in removing antibiotics due to the toxicity of the antibiotics [12]. Hence, among various treatment methods, AOPs is one of the most promising technologies in FLQ removal as they can mineralize the pollutants and

its relatively simple operation method when compared to other methods. Generally, AOPs involved the use of chemically generated reactive species (RS) for pollutant removal. Among various AOPs, sulfate based-AOP (SR-AOPs) have recently been gaining attention for water remediation due to its (i) relatively simple operation when compared to other type of AOPs (involved solid initiator, making its storage and transport relatively easier), (ii) high efficiency in degrading a myriad of persistent pollutants, and (iii) versatility in treatment method (there are many activation methods to achieve SR-AOPs).

Table 1.1: Advantages and disadvantages of various wastewater treatment methods.

Methods	Description	Advantages	Disadvantages
Adsorption	Use of adsorbate to adsorb pollutant	Simple operation methods	Equilibrium-reliable process, can generate secondary pollution
Membrane filtration	Reduce pollutant released by filtration	Simple operation methods	Membrane fouling, small molecules may pass through
Biodegradation	Microbial community in activated sludge degrade the pollutants	Does not involved hazardous chemicals	Slow treatment process, pollutant may be cytotoxic to the bacteria involved
AOPs	<i>In-situ</i> generation of reactive species for organics degradation	Relatively fast treatment time and can mineralize pollutants	Ineffective consumption of reactive species

SR-AOPs can be achieved through activation of peroxymonosulfate (PMS). In the reaction system, PMS is activated to form highly reactive species (e.g., $\text{SO}_4^{\cdot-}$, $\cdot\text{OH}$,

and $^1\text{O}_2$) which can be employed to degrade organic pollutants into innocuous compounds [13]. Generally, PMS can be activated by thermal activations, ultraviolet radiations, ultrasound, and homogeneous and heterogeneous catalysis [13, 14]. Among the activation methods, heterogeneous catalysis is the most preferable activation method as it does not involve external energy and the catalyst can be easily collected for subsequent uses or regeneration. The general RS generation and PMS activation mechanism will be discussed in **Chapter 2.1**.

Recently, carbonaceous catalysts (carbocatalysts) have gained a lot of attention for persulfate activation as carbocatalysts can avoid the use of metals, which are prone to metal leaching during applications. Some of the carbocatalysts used include graphene [15, 16], CNTs [17, 18], and biochar [19]. Among the various carbocatalyst, biochar is the most promising materials for catalysis purposes as it can be easily synthesized and functionalize, as well as promotes waste recovery. Generally, biochar can be produced through carbonization of biomass under inert condition. Among various biomass, lignocellulosic biomass (e.g., sawdust) was recently widely used as a carbon source for biochar production as it has high lignin content, which ensures good biochar yield [20]. As sawdust can give high biochar yield and its abundance as biowaste in Malaysia (due to the large timber industry in Malaysia [21]), it is favorable to use sawdust as a carbon precursors for preparing carbocatalyst for PMS activation applications.

One of the shortcomings of using carbocatalyst is its inertness. Without proper modification, carbocatalyst is generally inert towards redox reaction due to its lack of active sites. To break the inertness of the carbocatalyst, heteroatom doping (such as nitrogen (N), sulfur (S), phosphorus (P), boron (B)) into the carbocatalyst can be conducted to introduce active sites or alter the physiochemical characteristics of the

carbocatalyst [22]. For instance, introduction of N atoms into the carbon lattice can modulate and increase the charge density of the carbocatalyst due to the difference in electronegativity between N and carbon (C) atoms ($\chi_{\text{N}} = 3.04 > \chi_{\text{C}} = 2.55$). This can subsequently facilitate the PMS (negatively charged molecule) to approach the carbocatalysts for activation [23, 24]. Furthermore, heteroatom doping of B or S can introduce more active sites for PMS activation, further improving the performance for PMS activation [25, 26]. While single-heteroatom doping is effective in enhancing the PMS activation performance of the carbocatalysts, multi-heteroatom doping (combination of two or more heteroatoms) can further improve the catalytic activities of the carbocatalyst, outperforming single heteroatom doped carbocatalyst. The observed enhancement is due to the synergistic interaction between the heteroatom moieties, in which, the additional heteroatoms can redistribute the charge density of the carbon lattice, benefitting PMS activation [27, 28]. Hence, multi-heteroatom doped carbocatalyst can potentially be used as a PMS activator for FLQ removal.

Due to the great potential of using multi-heteroatom-doped carbocatalyst for PMS activation, this study will focus on preparation of N, S-, and N, B-co-doped biochar for FQL antibiotics removal. In this study, sawdust was chosen to be the carbon source due to its high lignin content and its availability in Malaysia. CIP and GAT antibiotics were chosen as the model FQL antibiotics due to their prevalence in various water bodies.

1.2 Problem statement and hypothesis

To improve the catalytic activity of the carbocatalyst, multi-heteroatom doping can be done to endow active sites and alter the surface chemistry of the carbocatalysts. Among various heteroatom combination, N, S- and N, B-co-doped carbocatalyst were shown to be very effective in PMS activation [29]. While these heteroatoms can

enhance the catalytic activities of the carbocatalyst, unoptimized synthesis methods/parameters may worsen the catalytic activities of the carbocatalyst. For instance, while favorable moieties such as graphitic N and thiophenic S in N, S-co-doped carbocatalyst can be formed in high synthesis temperature (>600 °C), excess heat treatment can lead to loss of heteroatoms, which may be detrimental for PMS activation [27, 30, 31]. Furthermore, incorporation of excess S heteroatoms into the carbocatalyst can decrease the overall surface charge, leading to lower PMS activation efficiency [32]. On the other hand, it is generally favorable to prepare N, B-co-doped carbocatalyst through sequential doping process as doping N and B simultaneously can prompt the formation of *h*-BN secondary phase which is catalytic inactive [28]. However, there are also study showing that doping N first can cause the formation of edge B-N bonds during subsequent B doping [33]. A more thorough discussion is provided in **Chapter 2.7**. In short, the properties of the multi-heteroatom-doped carbocatalyst can be tuned by different synthesis methods/parameters. Hence, more studies focusing on the optimization of synthesis methods/parameters and the heteroatom-doping mechanism are required to provide some understanding in designing effective carbocatalyst for SR-AOPs.

On the other hand, current understanding on the kinetics of pollutant removal is limited. Previous kinetic studies on pollutant removal in catalytic PMS system mostly involved pseudo-first order kinetics as the PMS concentration is assumed to be constant (excess in PMS) [34]. While this assumption is valid in certain cases, it is not useful for practical application, considering the PMS concentration cannot be in excess due to economic reasons. Wang and Wang [35] proposed a two-phase kinetics model which composed of fast and slow phases, with fast phase contributed by rapid formation of surface-bound active species to describe PMS activation by graphene

oxide and biochar. Furthermore, a second-order kinetics of PMS consumption was also described by Wang et al. [36]. However, while these studies have provided useful advancement, they only accounted for PMS consumption. A kinetic study that incorporates both PMS consumption and pollutant degradation may provide useful insights and should be explored.

Lastly, the emergence of nonradical pathway in PMS activation by multi-heteroatom-doped carbocatalysts may further complicates the reaction system. For instance, the degradation efficiency and pathways will be vastly different with the traditional AOPs, which mostly involved free radicals in organics mineralization [37, 38]. In multi-heteroatom-doped carbocatalyst, the interaction between the heteroatoms can alter the dominant PMS activation pathway (will be further discussed in **Chapter 2.5**). Hence, the PMS activation by the multi-heteroatom-doped carbocatalyst should be studied to gain insight on its reaction behaviour. Furthermore, the applicability of the multi-heteroatom-doped carbocatalyst in various water bodies and the degradation pathways of the pollutant are needed to ascertain the practicability of the carbocatalyst in treating real wastewater.

Overall, through careful optimization during the synthesis process, the multi-heteroatom-doped carbocatalyst is expected to be able to activate PMS effectively for FLQ antibiotics removal. Furthermore, we also expect that we can obtain some insights on the heteroatom doping mechanism of the carbocatalyst through studying the change carbocatalyst properties with varying synthesis parameters. Furthermore, through monitoring the change of concentration of the FLQ antibiotics and PMS, a kinetic model is expected to be developed. Lastly, multi-heteroatom-doped carbocatalysts are hypothesized to be effective in activating PMS for FLQ antibiotics degradation as they

can activate PMS with multiple pathways, providing versatilities in FLQ antibiotics removal.

1.3. Objectives and scope of study

The objectives of this study are:

1. To synthesize the multi-heteroatom-doped biochar (N, S-co-doped biochar, BSN-Ts, and N, B-co-doped biochar NB-BCs).
2. To characterize the BSN-Ts and NB-BCs using various characterization techniques.
3. To study the performance of BSN-Ts and NB-BCs as PMS activator for FLQ antibiotics removal in various operational parameters.
4. To develop a kinetic model and determine the PMS activation mechanism and the FLQ antibiotics degradation pathway by BSN-Ts and NB-BCs

This study was separated into the two parts. The first part of the study mainly focused on the preparation of N, S-co-doped biochar (BSN-Ts) at varying synthesis temperature and its performance as PMS activator for GAT removal. Furthermore, a kinetic model was developed based on GAT removal and PMS consumption. As N, B-co-doped carbocatalyst was not studied as extensively as with N, S-co-doped carbocatalyst in the past, the second part of the study was done to investigate the application of N, B-co-doped carbocatalyst (NB-BCs) as PMS activator for CIP removal. Kinetic modelling in this part of the study is omitted due to the complications by adsorption process. Furthermore, the PMS activation mechanism of BSN-Ts and NB-BCs was determined using chemical scavenging studies and electrochemical studies while the degradation pathway of FLQ antibiotics were proposed by identifying the degradation intermediates of the FLQ antibiotics.

1.4 Organization of thesis

This thesis comprises 6 chapters, namely (i) Introduction, (ii) Literature review, (iii) Materials and Research Methodology, (iv) Results and discussion (two chapters), and (v) Conclusions and Recommendation for Future Research.

Chapter 1: Introduction

This chapter provides the background knowledge of this study as well as discusses on the current knowledge gap and research motivation of this thesis. Furthermore, the research objectives and thesis organization are then outlined in this chapter.

Chapter 2: Literature Review

This chapter provides the relevant literature reviews that focused on the application of multi-heteroatom-doped carbocatalyst in PMS activation for water remediations. This chapter will start off by discussing the general PMS activation mechanism by the carbocatalyst and will follow up with a brief introduction on the common carbon allotropes used in PMS activation. The chapter will also briefly discuss on the characteristics of an efficient carbocatalysts and then will review the influence of heteroatoms in single- and multi-heteroatom doped on the electronic properties of the carbocatalysts. Lastly, the application of multi-heteroatom-doped carbocatalysts in PMS activation and the general considerations for N, S- and N, B-co-doped biochar preparation will be discussed.

Chapter 3: Materials and Research Methodology

This chapter gives a detailed account on the preparation of multi-heteroatom doped carbocatalyst. The details for the characterization studies and performance studies are also presented.

Chapter 4: Nitrogen, sulfur-co-doped carbocatalyst as peroxymonosulfate activator for gatifloxacin removal

This chapter describes the preparation and formation mechanism of N, S-co-doped carbocatalyst. The as-prepared carbocatalysts were then characterized to investigate the intrinsic and extrinsic properties of the carbocatalysts. The kinetic model for GAT removal via PMS activation by the carbocatalyst was developed. Lastly, the general PMS activation pathway and degradation pathway of GAT were presented.

Chapter 5: Nitrogen, boron-co-doped carbocatalyst as peroxymonosulfate activator for ciprofloxacin removal

This chapter describes the preparation of N, B co-doped carbocatalyst with varying sawdust:boric acid:urea ratio. The N, B co-doped carbocatalyst were characterized thoroughly to study the formation mechanism. The performance of N, B co-doped carbocatalysts as PMS activator for CIP removal were evaluated. Furthermore, the PMS activation mechanism and the degradation pathway of CIP were also outlined.

Chapter 6: Conclusions and recommendations

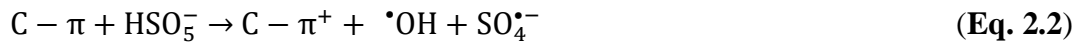
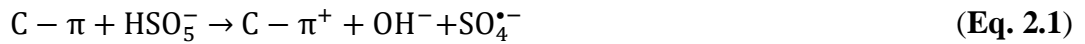
This chapter summarizes both of the studies from **Chapters 4** and **5**. Furthermore, recommendations for future works such as studies on structure-performance relationship of the multi-heteroatom-doped carbocatalyst, exploring other synthesis methods/parameters and applicability of multi-heteroatom-doped carbocatalyst are also outlined.

CHAPTER 2

LITERATURE REVIEW

2.1 Fundamentals of catalytic peroxymonosulfate activation

When PMS interacts with carbocatalyst, it can be activated to produce reactive species (RS) which can be employed to attack organic pollutants. Regardless of whether it is single-heteroatom- or multi-heteroatom-doped carbocatalyst, the PMS activation mechanisms generally proceeds through radical and nonradical pathways (shown in **Figure. 2.1**). In radical pathway, PMS directly participate in an electron transfer reaction with carbocatalyst to undergo peroxide bond cleavage, forming free radicals ($\text{SO}_4^{\bullet-}$ and $\bullet\text{OH}$). The oxidized active sites may react with another PMS to form less reactive radicals such as $\text{SO}_5^{\bullet-}$, restoring its original form for further reaction [13, 39]. Typically, it has been reported that the radical pathway may occur at either the defective sites of the carbocatalyst, Lewis base sites such as ketonic group and pyrrolic/pyridinic N, or activated π electron in the sp^2 carbon lattice [15]. For instance, the π electron in the defective sites can catalyze PMS activation through the following reactions ((**Eq. 2.1**), (**Eq. 2.2**), (**Eq. 2.3**)):



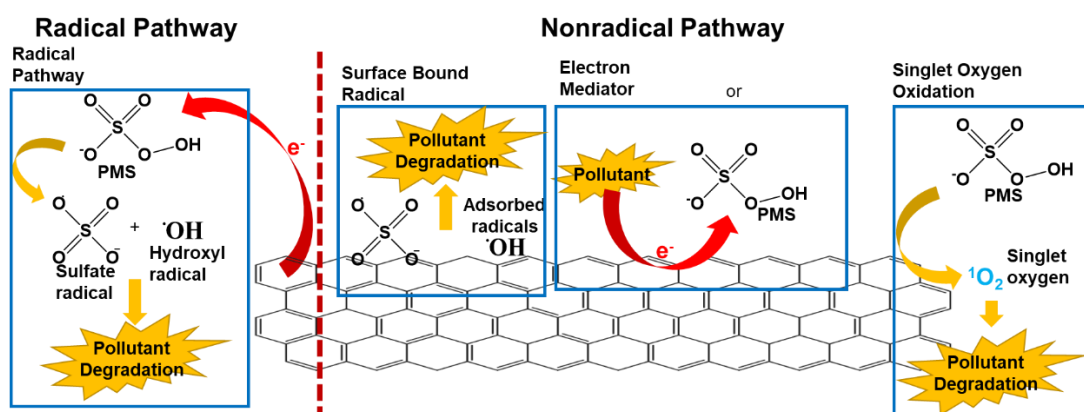


Figure 2.1. Reaction mechanism involving radical and nonradical pathway during PMS activation.

On the other hand, nonradical pathway involves surface bound radicals, electron mediation mechanism, and $^1\text{O}_2$ generation. In most cases, the carbocatalyst acts as a platform to facilitate the electron transfer reaction from PMS to pollutant and vice versa. The surface bound radicals (surface bound $\text{SO}_4^{\cdot-}$ and $\cdot\text{OH}$) are generated on the surface of the carbocatalyst and have restricted movement but reactive towards organic pollutants in close proximity. Electron mediation mechanism generally proceeds with (i) formation of catalyst-PMS complex (at electron deficient site), (ii) adsorption of organic pollutants on the catalyst (electron rich such as dopant site), (iii) redox reaction with organic pollutant undergoing oxidation (electron donor) while PMS undergoes reduction (electron acceptor) with electron transfer through the carbocatalyst as the electron mediator. Meanwhile, the $^1\text{O}_2$ generation during PMS activation can proceed via (i) reaction of PMS with ketonic group, (ii) self-decaying through combination of HSO_5^- and SO_5^{2-} , and (iii) formation of SO_5^{2-} through oxidation of PMS then subsequently react with water to produce $^1\text{O}_2$ [40, 41].

2.2 Carbocatalyst

Recently, various carbon allotropes were studied for PMS activation. **Figure 2.2** illustrates the structure of different carbon allotropes. Generally, crystalline carbon

such as reduced graphene oxide (rGO), carbon nanotubes (CNTs), ordered mesoporous carbon (OMC), and nanodiamonds were showed to be able to activate PMS effectively. This section will introduce the carbon allotropes used in PMS activation applications.

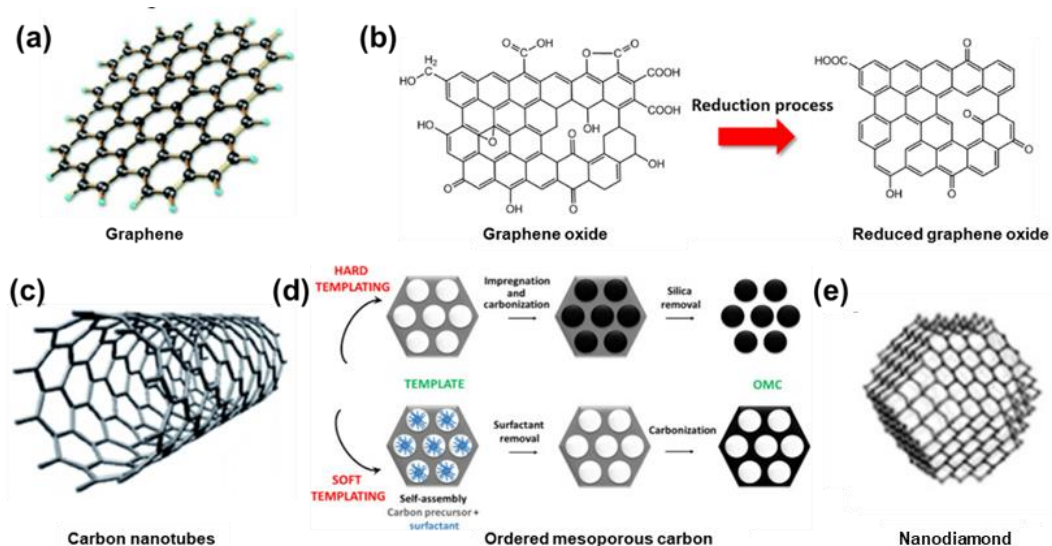


Figure 2.2. The structures of various carbon allotropes, (a) graphene, (b) reduction process from graphene oxide to reduced graphene oxide, (c) carbon nanotubes, (d) synthesis of ordered mesoporous carbon by using template route, and (e) nanodiamond. Reproduced with permission from [22, 42-44]

2.2.1 Graphene-based materials

Graphene-based materials such as graphene oxide (GO) and rGO were widely studied for PMS activations. These graphene materials can be synthesized with relatively simple synthesis method (Hummer's method) and they possess excellent physiochemical properties such as having large surface area and can be easily tuned by heteroatom doping. Graphene-based material possess conjugated π -system, which allows electrophilic attack of the pollutant [15]. However, pristine graphene or GO is generally chemically inert due to the lack of active sites and hence, post treatment such

as reduction of GO or heteroatom doping can be done to introduce defects and various functional groups for PMS activations. For instance, Sun et al. [16] showed that rGO with high defective degree induced by reduction of GO is able to outperform GO, activated carbon and also conventional Co_3O_4 catalyst for pollutant (phenol, 2,4-dichlorophenol and methyl blue) removal by PMS activation. Furthermore, various oxygen functional group such as COOH and C=O in graphene can also serve as the active sites for PMS activation [43]. Heteroatom doping of graphene-based material is shown to greatly enhance PMS activation by introducing more active sites for redox reactions [15]. For instance, Liang et al. [45] produced N-doped graphene through pyrolysis of metal organic framework and found that the carbocatalyst outperformed various metal-based catalyst such as Fe_2O_4 , Fe_3O_4 , MnO_2 , and Co_3O_4 for phenol removal by PMS activation. These results showed that proper functionalization of graphene is vital to produce high performance carbocatalyst for organic degradation in SR-AOPs.

2.2.2 Carbon nanotubes

CNT is composed sp^2 carbon network wrapped in a cylindrical geometry. Furthermore, the robust graphitized structure of CNT can give rise to good electrical conductivity and also allow various alterations on the electrical properties of CNT through functionalization (with defects, oxygen functional groups and heteroatoms) for PMS activation [46-48]. Previously, Chen et al. [17] used CNTs to activate PMS for AO7 removal and found that CNTs can activate PMS through both radical and nonradical pathways. The reactivity of the CNT can also be enhanced through post-treatment of the CNT. For example, Han et al. [18] showed that the reaction pathways and reactivity of CNT in PMS activation can be modulated through endowing C=O groups *via* acid-thermal treatment of CNT. Furthermore, various heteroatom-doped

CNT were shown to be very effective in activating PMS [49-51]. For instance, N doping of CNT was shown to improve the PMS adsorption capability for formation of PMS-carbocatalyst complex, allowing the electron transfer mechanism to occur [52]. In general, CNTs possess unique electronic property which allows various modifications that benefits PMS activation. However, synthesis of pristine CNTs is generally hard and usually require more sophisticated and delicate synthesis method such as chemical vapour deposition, laser ablation, and arc discharge [53].

2.2.3 Ordered mesoporous carbon

OMCs consist of 3D multi-hollow carbon structure with pore sizes ranging from 2 nm to 5 nm. Due to its highly uniformed structure and porous nature, OMC were widely used as adsorbent, catalyst support as well as catalysis [54-56]. OMCs are generally fabricated through hard/soft templating approach and are generally hard to functionalized due to its high crystalline structure [57]. In SR-AOPs, Wang et al. [25] employed B-doped OMC and found that presence of oxidized B group (BC_2O and BCO_2) can facilitate formation of 1O_2 for organics removal. Sun et al.[58] also employed N, S-co-doped OMS prepared through pyrolysis of thiourea and urea with CMK-3 at 350 °C and showed that it can activate PMS through 1O_2 formation and electron mediation mechanism. Although OMCs are capable to activate PMS effectively, functionalization of OMCs is generally difficult and required more delicate methods to preserve its 3D structure. For instance, post-treatment of OMC can lead to destruction of ordered structure, which will decrease the SSA and total pore volume and subsequently lead to poorer catalytic performance [23]. Furthermore, OMCs are usually fabricated through hard/template approach, which required acid etching for template removal, making the synthesis procedures of OMCs to be more complex and costly.

2.2.4 Nanodiamond

Nanodiamond (ND) is composed of sp^2 carbon engulfing the sp^3 core. Recently, ND has been attracting researchers for PMS activation application [59, 60]. Duan et al. [59] found that increasing the sp^2 thickness around the ND can facilitate nonradical pathway by enhancing PMS adsorption and simultaneously reduce the overall charge transfer between the ND and PMS. Furthermore, Duan et al. [61] used N-modified ND for effective phenol removal through PMS activation, outperforming other carbocatalysts such as fullerene, CNTs and other graphene-based materials. Despite its effectiveness in PMS activations, NDs are generally more expensive and are resistance towards chemical modification due to its high stability. Several methods for functionalization of ND include thermal annealing at very high temperature (~ 1000 °C) [59, 60, 62] or using catalysts such as $FeCl_3$ to facilitate surface graphitization [63].

2.2.5 Amorphous Carbon

Recently, amorphous carbons such as activated carbon and biochar were used in PMS activation. Due to their lack of crystallinity, they are easier to be functionalized when compared with other carbon allotropes with high crystallinity that required more delicate approaches for chemical modifications. Typically, amorphous carbon can be obtained through carbonization of carbon source (biomass/ionic liquid) and functionalized by mixing the carbon source with desired dopant precursors or activator in the carbonization process. Biochar is widely used for PMS activation as the precursors are originated from biowaste and can be easily obtained. As the characteristics of biomass from different sources are vastly different, it allows a much flexible way in tuning the physiochemical properties of the biochar. Furthermore, the biochar properties can be modulated with various synthesis parameters such the carbon source, synthesis temperature, heating rate, and holding time during char formation

[19]. For instance, higher ketonic O (C=O) content is beneficial for persulfate activation and can be obtained through pyrolysis of biochar with biomass that has high cellulose:lignin content of the biomass [64]. Self-doping of biochar can also be achieved through pyrolysis of biomass with high percentage of respective heteroatoms without additional heteroatom dopant. For instance, several biomasses such as ginkgo leaves [65] and human hair [31] were used to prepare N, S-co-doped biochar without addition of external N and S dopants. Despite its flexibilities, amorphous carbon possesses lower chemical resistance towards oxidative environment, which will lead to poorer reusability when compared to other crystalline carbon allotropes [66].

2.3 General properties of carbocatalyst for PMS activation.

After discussing the carbon allotropes in PMS activation applications, this section will discuss the on general properties of efficient carbocatalyst as PMS activator. Some of the physiochemical properties that affect the efficiency of the carbocatalyst for PMS activation include (i) specific surface area (SSA) and porosity, (ii) surface defects/graphitization, and (iii) surface functionalities. **Table 2.1** summarizes the characteristics and the strategies for improving the catalytic activity of the carbocatalyst.

Typically, higher SSA is beneficial for PMS activation as higher SSA maximize the exposure of active sites for adsorption and PMS activation. Furthermore, larger pore volume and abundant of meso- and micropores in carbocatalyst can increase SSA and also induce more edge defects [67]. Meanwhile, higher surface defects are desirable for catalysis because the surface defects can host active sites for both adsorption and PMS activation [43, 68, 69]. For instance, defects (vacancies) formed through deliberate heteroatom removal by high synthesis temperature were shown to facilitate PMS adsorption [70, 71]. However, too much surface defect may

impair surface conductivity (lower graphitization) and lower, which might be detrimental for PMS activation.

On the other hand, higher degree of graphitization promotes better electron conductivity, which permits nonradical pathways such as electron transfer pathway. For instance, Feng et al. [72] showed biochar with higher graphitization facilitate electron mediator mechanism with the biochar acting as the electron mediator. Furthermore, graphitized structure can enhance pollutant (with aromatic ring) adsorption through π - π interaction, further facilitate electron transfer between the pollutant and the carbocatalyst for electron transfer pathway [73].

The surface functionalities such as oxygen functional group and heteroatom moieties can significantly affect the overall performance of the carbocatalyst for PMS activation. For oxygen functional group, Lewis bases such as ketonic group were deemed as favorable active sites for PMS activation. For instance, various computational and experiment studies have suggested that ketonic group can effectively aid in PMS adsorption and activation by allowing electron transfer from the ketonic group to the PMS molecules [74, 75]. However, excessive O moieties (even with ketonic O) can deteriorate the PMS activation efficiency of the carbocatalyst due to the impaired surface conductivity and strong PMS-carbocatalyst interaction, preventing PMS from releasing ROS for organics degradations [75]. On the other hand, heteroatom-doping can introduce more active sites and can cause more direct and profound changes on the charge and spin density of the carbocatalyst. Owing to the fact that heteroatom doping can effectively affect the chemical properties of the carbocatalyst, the effect of heteroatom-doping will be deeply discussed in **Chapter 2.4** and **2.5**.

Table 2.1. Characteristics of catalyst and enhancement strategies for improved catalytic activity.

Characteristics	Description	Ways to enhance
Atomic charge/Charge density	<ul style="list-style-type: none"> Positive/negative charge density of the carbon lattice can facilitate better adsorption 	<ul style="list-style-type: none"> Heteroatom doping
Spin density and surface conductivity	<ul style="list-style-type: none"> The spin density can be linked to the density of active sites Surface conductivity reflects electron mobility and can facilitate adsorption 	<ul style="list-style-type: none"> Heteroatom doping Synthesis parameter
Defects and active sites	<ul style="list-style-type: none"> Defects can disrupt the inertness of sp^2 lattice and serve to host active site for PS activation Higher active sites promote better catalytic activity 	<ul style="list-style-type: none"> Heteroatom doping Oxidation Selecting suitable dopant precursor Template-based synthesis
Specific surface area	<ul style="list-style-type: none"> Large surface area exposes active sites for 	<ul style="list-style-type: none"> Selecting suitable dopant precursor

- adsorption and redox reaction
- Template-based synthesis
- Chemical activation

2.4 Effects of single heteroatom-doped carbocatalyst in PMS activation

Generally, doping of carbocatalyst with single heteroatom such as N, B, P and S can cause disturbance in the conjugated carbon network. Furthermore, presence of heteroatom can introduce various surface moieties, which can be conducive for PMS activation. **Figure 2.3** summarizes the effect of various heteroatoms on PMS activation. From **Figure 2.3**, the presence of heteroatom generally can endow more active sites and polarize the surface charge of the carbocatalyst.

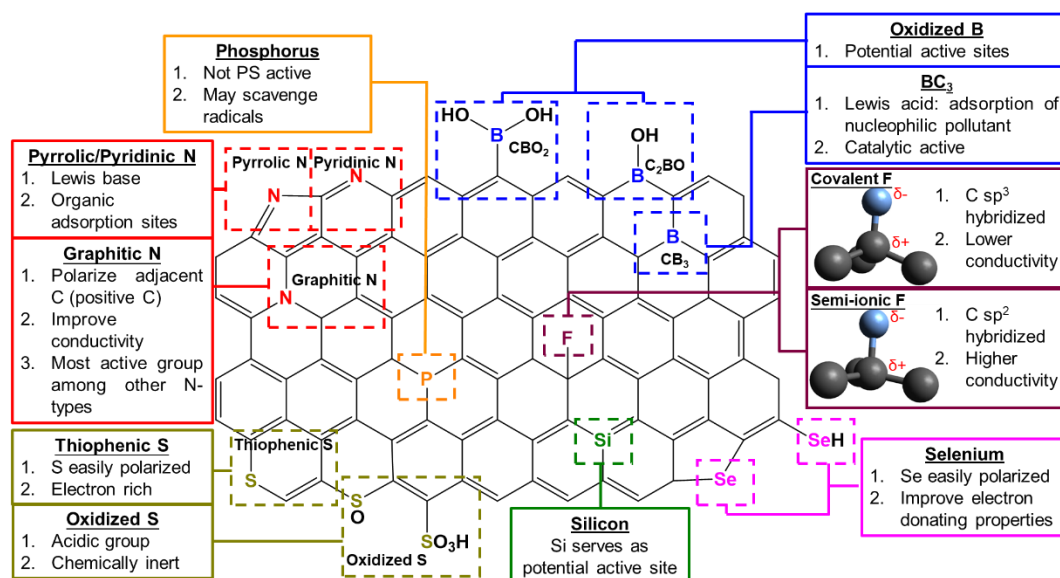


Figure 2.3. Effect of various heteroatoms on PMS activation

2.4.1 Nitrogen doping

When N atom is doped into the carbocatalyst, it can adopt bonding configurations of oxidized N, graphitic N, pyrrolic N, and pyridinic N [76]. Generally,

presence of these N moieties (except oxidized N) can polarize neighbouring carbon which enhance interaction between PMS/pollutant and carbocatalyst. Graphitic N is formed through substitution of carbon with N in the carbon network. Apparently, the presence of N moieties, particularly N, has been associated with improved adsorption of PMS and aromatic compounds [77], where these N moieties can facilitate adsorption via Lewis acid-base interaction. Graphitic N can contribute one electron to the conjugated π electron system, which will activate the π electron and improve electron transfer from the carbocatalyst to PS. Furthermore, graphitic N can lead to high electron deficiency around adjacent C, promoting PMS adsorption and activation [23, 78]. Theoretical study indicated that graphitic N has the lowest PMS adsorption energy due to the ability of N to tailor the charge distribution of surrounding carbon atoms [47]. Graphitic N has been identified as the active site for both radical and nonradical pathways [24].

On the other hand, pyridinic N has N atom bonded to a 6-member carbon rings and can donate its π -electron to the conjugated carbon network, which can in turn increase the electron donating properties. Pyrrolic N has N atom bonded to a 5-member carbon ring. Pyrrolic N has a lower basicity than pyridinic N and less reactive when compared to pyridinic N [79]. Both pyrrolic and pyridinic N possess unpaired electron that are not delocalized into the π system and can facilitate electron mediation mechanism [23, 36, 80]. The edge N moieties, especially pyrrolic N, has been reported to facilitate peroxydisulfate (PDS) activation (potentially PMS) through electron mediation mechanism where PDS is reduced at the pyrrolic group while pollutant reacts at the adjacent electron deficient C atoms [36] Apparently, graphitic N is more redox active than pyridinic and pyrrolic N as evidence in various experimental and theoretical results [52, 81, 82]. This may due to the greater influence of graphitic N in

altering the charge density of the carbon structure as graphitic N is bonded with three carbon atoms whereas pyridinic N and pyrrolic N are bonded with only two carbon atoms [79].

2.4.2 Boron doping

Typically, B doping on carbocatalyst can induce the formation of BC_3 and oxidized B (CBO_2 and C_2BO), endowing the carbocatalyst with PMS activation functionality [15]. Having only three valence electrons, incorporation of B into the carbon lattice will perturb the electronic structure in the carbon system. Being electron deficient, B can act as both π -electron and acceptor a σ -electron donor due to its lower electronegativity of B when compared to carbon ($\chi_C = 2.55 > \chi_B = 2.04$) [83]. These attributes can cause activation of π -electrons surrounding B and the neighbouring C, introduce “hole” that facilitates charge mobility, and improve conductivity of the doped carbon [83]. BC_3 moiety which is formed through B substituting the carbon atom in the sp^2 carbon structure has been shown to be the best bonding configuration to improve the catalytic activity of the carbocatalyst. Meanwhile, the CBO_2 and C_2BO moieties permit PS activation through the nonradical pathway involving the formation of 1O_2 or surface-confined complex during PS activation [25, 84]. Furthermore, B can also act as a Lewis acid, which can promote interaction of nucleophilic molecules with the carbocatalyst, facilitating PMS and pollutant adsorption [85]. It has been reported that B-doped carbon can facilitate the adsorption of PMS and various pollutants including sulfamethoxazole and tetracycline through π - π interaction, hydrogen bond formation, pore filling, and electrostatic interaction, benefiting PMS activation [85, 86].

2.4.3 Phosphorus doping

Being in the same group with N, P has the same number of valence electrons and can act as an n-type dopant by introduction extra electrons after doping into the carbon structure. P has lower electronegativity and larger atomic size when compared with N, making P a relatively better electron donor to the conjugated carbon system [87]. Hence, P doping can induce charge delocalization around the carbon lattice while simultaneously forming more defective sites surrounding the carbon structure. P doping is also expected to improve the oxidation resistance of the carbocatalyst by inducing negative charge to the surrounding carbon atoms, creating electron cloud to shield the carbon lattice from intense oxidation environment [88]. Furthermore, P doping is also expected to increase the adsorption capacity of the carbon for various pollutants through the formation of π - π interaction, hydrogen bond formation and donor-acceptor interaction [89]. However, the use of P-doped carbocatalyst for PMS activation is less explored which may due to its poor reactivity towards PMS activation. Furthermore, it is also reported that P moieties can scavenge $\cdot\text{OH}$ (and possibly $\text{SO}_4^{\cdot-}$), leading to unproductive radical consumption [90].

2.4.4 Sulfur doping

S has a relatively larger size compared with carbon and can generally form thiophenic S and oxidized S during S doping. The presence of thiophenic S is beneficial for PMS activation as the S atom is electron-rich and may serve as a potential active site for PMS activation via radical to generate $\cdot\text{OH}$ and $\text{SO}_4^{\cdot-}$ [26, 91]. Furthermore, thiophenic S can induce defects and alter the spin and charge density around the neighboring carbon, facilitating PMS activation [92, 93]. Meanwhile, oxidized S is generally considered to be acidic groups and possess a certain degree of electron withdrawing properties that can limits electron transfer to PMS for activation [92, 94].

Excessive S doping may inhibit the adsorption performance [94], potentially leading to poorer catalytic activity.

2.4.5 Others

Other heteroatoms such as halogen (F, Cl, Br, and I) can also be doped into the carbocatalyst. Due to the large electronegativity difference between halogen and carbon, the formation of C-halogen bond can polarize adjacent carbon and improve overall electronic properties of the carbon structure. Among the halogens, F doping is the most favorable halogen dopant as it provides the largest electronegativity difference with carbon, causing the greatest polarization of the carbon structure. When F is doped, it can be bonded ionically, semi-ionically, or covalently. The reactivity of C-F bond increases in the order of covalent < semi-ionic C-F < ionic C-F bond due to the higher polarizing ability of semi-ionic and ionic C-F bonds [95-98]. However, the applicability of halogen-doped carbocatalyst as PMS activator is limited due to its relatively lower stability as the halogen tends to undergo substitution reactions. Besides halogen, Se and Si have also been doped into the carbocatalyst to form C-Se and C-Si moieties, respectively. Se is easily polarized and able to introduce defects to the carbocatalyst due to its relatively large atomic size when compared to carbon [99]. Furthermore, Se can also enhance the electron-donating properties of the carbocatalyst, making it suitable for persulfate activation [100]. Meanwhile, Si doping into the carbocatalyst showed enhanced catalytic activity for CO₂ reduction [101], NO reduction [102], and oxygen reduction reaction (ORR) [103] (and potentially PMS) due to its improved ability in adsorbing and interacting with the respective molecules.

2.5 Effect of multi-heteroatom-doped carbocatalyst in PMS activation

The presence of two or more heteroatoms in the carbon structure can induce profound changes to the electronic properties of the carbocatalyst, altering the